JOC Article

Facile Synthesis and Characterization of Naphthidines as a New Class of Highly Nonplanar Electron Donors Giving Robust Radical Cations

Christophe Desmarets,[†] Benoît Champagne,[§] Alain Walcarius,*[,‡] Christine Bellouard,[||] Rafik Omar-Amrani,[†] Abdelaziz Ahajji,[⊥] Yves Fort,[†] and Raphaël Schneider*[,†]

Synthèse Organométallique et Réactivité, UMR 7565, Faculté des Sciences, BP 239, 54506 Vandoeuvre les Nancy, France, Laboratoire de Chimie Physique et Microbiologie pour l'Environnement, UMR 7564, CNRS - Université Henri Poincaré Nancy I, 405 rue de Vandoeuvre, 54600 Villers-les-Nancy, France, Laboratoire de Chimie Théorique Appliquée, FUNDP, Rue de Bruxelles 61, 5000 Namur, Belgium, Laboratoire de Physique des Matériaux, UMR 7556, Faculté des Sciences, BP 239, 54506 Vandoeuvre les Nancy, France, and Laboratoire d'Etudes et de Recherche sur le Matériau Bois, UMR 1093, Faculté des Sciences, BP 239, 54506 Vandoeuvre les Nancy, France

raphael.schneider@sor.uhp-nancy.fr

Received August 18, 2005

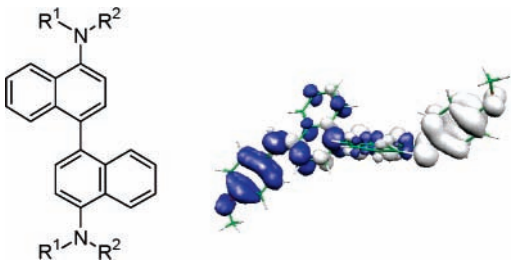

Naphthidines **2** were prepared by nickel-catalyzed amination of 1-chloronaphthalene followed by oxidative homocoupling of 1-naphthalene amines **1** using titanium(IV) tetrachloride. The electronic and magnetic properties of materials **2** were investigated by cyclic voltammetry and other electrochemical techniques, EPR and UV−visible spectroscopies, and magnetic susceptibility. It was demonstrated that compounds **2** could be easily and reversibly oxidized via a two-electron-transfer reaction into their bis(radical cation) $\mathbf{2}^{2.2+}$, which displays a substantial stability at room temperature (the half-life of $\mathbf{2}^{2.2+}$ estimated by EPR at 25 °C was 10 days). B3LYP/6-31G* optimized structures of *N*,*N*′-bis(4-methoxyphenyl)-(1,1′-binaphthyl)-4,4′-diamine **2g** shows significant differences in the torsion angle between the naphthalene moieties depending on its oxidation state. Twisted structures are preferred for neutral compounds, whereas more planar are favored for the oxidized forms $\mathbf{2g}^{\bullet+}$ and $\mathbf{2g}^{2.2+}$ to realize spin and/or charge delocalizations over the whole π-system. Such conformation changes concerted with the electron transfers contribute to explain the unusual two-electron process observed in the electrochemical behavior of **2g** instead of the two single-electron transfers that would have been expected in the case of two successive oxidations. It is finally shown that the oxidation of **2g** in CH_2Cl_2 with thianthrenium perchlorate ($ThClO_4$) generates the dication $\mathbf{2g}^{2.2+}$ with singlet spin-multiplicity.

Introduction

Conjugated organic materials (both low molecular weight compounds and polymers) have recently received much attention due to their potential applications in organic light-emitting diodes (OLEDs), field effect transistors, charge storage devices, photodiodes, sensors, etc.[1] These organic electroactive and photoactive materials are usually based on thiophene, pyrrole, carbazole, or arylamine moieties. In the case of arylamines, a great number of studies were devoted to 1,4-phenylenediamines[2] and 4,4′-diaminobiphenyls[3] because these unique families of materials are highly electron-rich and can produce delocalized

[†] UMR 7565, Faculté des Sciences.
[‡] UMR 7564, CNRS - Université Henri Poincaré Nancy I.
[§] FUNDP.
[||] UMR 7556, Faculté des Sciences.
[⊥] UMR 1093, Faculté des Sciences.

10.1021/jo0517444 CCC: $33.50 © 2006 American Chemical Society
Published on Web 01/19/2006

radical cations. Compared to 1,4-phenylenediamines and 4,4′-diaminobiphenyls, which have found wide applications in OLEDs due their high stability in the oxidized form, binaphthyl conjugated aromatic amines have been much less studied, although naphthalene, 1,4- or 1,5-ethylnylnaphthalene, or binaphthyl-based oligomers were developed as spacers or connectors[4] in studies dealing with energy transfer.[5]

Among the physical properties sought in new materials, especially for application in OLEDs, is their thermal and morphological stability. Amorphous materials possessing high glass transition temperatures (T_g) should have better opportunity for retaining the film morphology during device operation. A very simple concept for the formation of amorphous glass is nonplanar molecular structure, because easy packing of molecules and hence ready crystallization can be retarded. Nonplanar configuration has been achieved with the use of star-shaped molecules[6] or incorporation of bulky moieties in the molecules.[7] As a result of the rotation barrier around the central carbon−carbon bond and the torsion angle between the naphthyl units, naphthidines may constitute attractive systems to study switching phenomena in organic redox systems and therefore for the development of efficient hole-transport materials.

However, because of the lack of suitable methods for the synthesis of naphthidines, their hole-transport properties have not been studied thoroughly even though good efficiencies should be attained with these compounds. *N,N,N′,N′*-Tetramethylnaphthidine (TMN),[8,9] *N,N′*-diphenylnaphthidine,[10] and the parent 5,5′-di(8-aminoquinoxalyl)[11] are the sole compounds containing a binaphthyl core or a heterocyclic analogue core structure described in the literature. The synthesis of the former compounds has mainly been achieved by oxidative dimerization using CrO_3[10a] or $TiCl_4$[9] of the corresponding naphthylamines. Although the reported methods are, in principle, applicable to *N*-substituted naphthylamines, such procedures have not been reported yet. Other methods involving anodic oxidation followed by electrodimerization of *N,N′*-dimethyl-1-naphthylamine have also been described, but the yields are poor (30−35%) because the dimeric product is more readily oxidized than the starting material.[8] The use of a two-phase $H_2O-C_6H_5NO_2$ solvent system for the electrochemical oxidation was reported to overcome this difficulty, but no isolated yield is reported.[12]

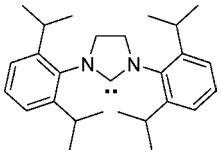

FIGURE 1. Structure of the SIPr ligand.

In this paper, we first report the synthesis of a series of *N,N′*-substituted naphthidines **2** using the nickel-catalyzed aryl amination methodology we recently established.[13,14] The electronic and magnetic properties of these materials were next investigated by several electrochemical techniques (cyclic voltammetry, chronoamperometry, coulometry), EPR and UV−vis spectroscopies, and magnetic susceptibility, as well as quantum chemical calculations within the density functional theory (DFT) approach.

Results and Discussions

Synthesis. Preparation of naphthidines **2** was carried out by the two-step synthetic procedure starting from 1-chloronaphthalene as shown in Scheme 1.

We have recently reported the use of a Ni(0) catalyst associated with a strong electron-donating and sterically hindered *N*-heterocyclic carbene[15] (*N,N′*-bis(2,6-diisopropylphenyl)-dihydroimidazol-2-ylidene, SIPr) (Figure 1) to allow mild amination of aryl chlorides with several classes of amines.[14] We first investigated the scope and limitations of this catalyst system for the cross-coupling of 1-chloronaphthalene with structurally and electronically diverse amines using the aryl

(1) (a) Leclerc, M.; Faïd, K. *Adv. Mater*. **1997**, *9*, 1087. (b) *Handbook of Conducting Polymers*, 2nd ed.; Skotheim, T. A., Elsenbaumer, R. L., Reynolds, J. R., Eds.; Marcel Dekker: New York, 1998. (c) *Advances in Synthetic Metals: Twenty Years of Progress in Science and Technology*; Bernier, P., Lefrant, S., Bidan, G., Eds.; Elsevier: Lausanne, 1999. (d) Leclerc, M. *J. Polym. Sci., Polym. Chem*. **2001**, *39*, 2867.

(2) (a) Deuchert, K.; Hünig, S. *Angew. Chem., Int. Ed. Engl*. **1978**, *17*, 875. (b) Louie, J.; Hartwig, J. F. *J. Am. Chem. Soc*. **1997**, *119*, 11695. (c) Wienk, M. M.; Janssen, R. A. J. *J. Am. Chem. Soc*. **1997**, *119*, 4492. (d) Nelsen, S. F.; Tran, H. Q.; Nagy, M. A. *J. Am. Chem. Soc*. **1998**, *120*, 298. (e) Schumann, J.; Kanitz, A.; Hartmann, H. *Synthesis* **2002**, *9*, 1268. (f) Yano, M.; Ishida, Y.; Aoyama, K.; Tatsumi, M.; Sato, K.; Shiomi, D.; Ichimura, A.; Takui, T. *Synth. Met.* **2003**, *137*, 1275. (g) Kim, M.-J.; Seo, E.-M.; Vak, D.; Kim, D.-Y. *Chem. Mater*. **2003**, *15*, 4021.

(3) (a) Suzuki, T.; Okubo, T.; Okada, A.; Yamashito, Y.; Miyashi, T. *Heterocycles* **1993**, *35*, 395. (b) Lambert, C.; Nöll, G. *Angew. Chem., Int. Ed*. **1998**, *37*, 2107. (c) Lambert, C.; Nöll, G. *J. Am. Chem. Soc.* **1999**, *121*, 8434. (d) Goodson, F. E.; Hauck, S. I.; Hartwig, J. F. *J. Am. Chem. Soc*. **1999**, *121*, 7527. (e) Hreha, R. D.; George, C. P.; Haldi, A.; Domercq, B.; Malagoli, M.; Barlow, S.; Brédas, J.-L.; Kippelen, B.; Marder, S. R. *Adv. Funct. Mater*. **2003**, *13*, 967. (f) Huang, Q.; Evmenenko, G.; Dutta, P.; Marks, T. J. *J. Am. Chem. Soc*. **2003**, *125*, 14704. (g) Low, P. J.; Paterson, M. A. J.; Puschmann, H.; Goeta, A. E.; Howard, J. A. K.; Lambert, C.; Cherryman, J. C.; Tackley, D. R.; Leeming, S.; Brown, B. *Chem. Eur. J*. **2004**, *10*, 83.

(4) (a) Chow, H.; Ng, M. *Tetrahedron: Asymmetry* **1996**, *7*, 2251. (b) Chow, H.; Ng, M. *Tetrahedron Lett.* **1996**, *37*, 2979. (c) Rodriguez, J. G.; Tejedor, J. L. *J. Org. Chem*. **2002**, *67*, 7631.

(5) (a) El-Ghayoury, A.; Harriman, A.; Khatyr, A.; Ziessel, R. *Tetrahedron Lett.* **1997**, *38*, 2471. (b) El-Ghayoury, A.; Harriman, A.; Khatyr, A.; Ziessel, R. *J. Phys. Chem. A* **2000**, *104*, 1512. (c) El-Ghayoury, A.; Harriman, A.; Khatyr, A.; Ziessel, R. *Angew. Chem., Int. Ed*. **2000**, *39*, 185.

(6) (a) Shirota, Y.; Kobata, T.; Noma, N. *Chem. Lett.* **1989**, 1145. (b) Higuchi, A.; Inada, H.; Kobata, T.; Shirota, Y. *Adv. Mater*. **1991**, *3*, 549. (c) Inada, H.; Shirota, Y. *J. Mater. Chem*. **1993**, *3*, 319. (d) Kuwabara, Y.; Ogawa, H.; Inada, H.; Noma, N.; Shirota, Y. *Adv. Mater*. **1994**, *6*, 677. (e) Katsuma, K.; Shirota, Y. *Adv. Mater*. **1998**, *10*, 223. (f) Wu, I.-Y.; Lin, J. T.; Tao, Y.-T.; E. Balasubramaniam, E. *Adv. Mater*. **2000**, *12*, 668.

(7) (a) Noda, T.; Ogawa, H.; Noma, N.; Shirota, Y. *J. Mater. Chem*. **1999**, *9*, 2177. (b) Wang, S.; Oldham, W. J., Jr.; Hudack, R. A., Jr.; Bazan, G. C. *J. Am. Chem. Soc*. **2000**, *122*, 5695.

(8) (a) Miras, M. C.; Silber, J. J.; Sereno, L. *Electrochim. Acta* **1998**, *33*, 851. (b) Zon, M. A.; Fernandez, H. *J. Electroanal. Chem*. **1990**, *295*, 41.

(9) Periasamy, M.; Jayakumar, K. N.; Bharati, P. *J. Org. Chem*. **2000**, *65*, 3548.

(10) (a) Braid, M. U.S. Patent 3,759,996, 1973. (b) Hornback, J. M.; Gossage, H. E. *J. Org. Chem*. **1985**, *50*, 541.

(11) Suzuki, T.; Saito, M.; Kawai, H.; Fujiwara, K.; Tsuji, T. *Tetrahedron Lett*. **2004**, *45*, 329.

(12) Vettorazzi, N.; Fernandez, H.; Silber, J. J.; Sereno, L. *Electrochim. Acta* **1990**, *35*, 1081.

(13) (a) Brenner, E.; Fort, Y. *Tetrahedron Lett.* **1998**, *39*, 5359. (b) Brenner, E.; Schneider, R.; Fort, Y. *Tetrahedron* **1999**, *55*, 12829. (c) Brenner, E.; Schneider, R.; Fort, Y. *Tetrahedron Lett.* **2000**, *41*, 2881. (d) Desmarets, C.; Schneider, R.; Fort, Y. *Tetrahedron Lett*. **2000**, *41*, 2875. (e) Desmarets, C.; Schneider, R.; Fort, Y. *Tetrahedron Lett*. **2001**, *42*, 247. (f) Desmarets, C.; Schneider, R.; Fort, Y. *Tetrahedron* **2001**, *57*, 7657. (g) Brenner, E.; Schneider, R.; Fort, Y. *Tetrahedron* **2002**, *58*, 6913. (h) Desmarets, C.; Schneider, R.; Fort, Y.; Walcarius, A. *J. Chem. Soc., Perkin Trans. 2* **2002**, 1844.

(14) (a) Gradel, B.; Brenner, E.; Schneider, R.; Fort, Y. *Tetrahedron Lett*. **2001**, *42*, 5689. (b) Desmarets, C.; Schneider, R.; Fort, Y. *J. Org. Chem*. **2002**, *67*, 3029. (c) Omar-Amrani, R.; Thomas, A.; Brenner, E.; Schneider, R.; Fort, Y. *Org. Lett*. **2003**, *5*, 2311. (d) Omar-Amrani, R.; Schneider, R.; Fort, Y. *Synthesis* **2004**, 2527.

SCHEME 1. Synthesis of Naphthidines 2

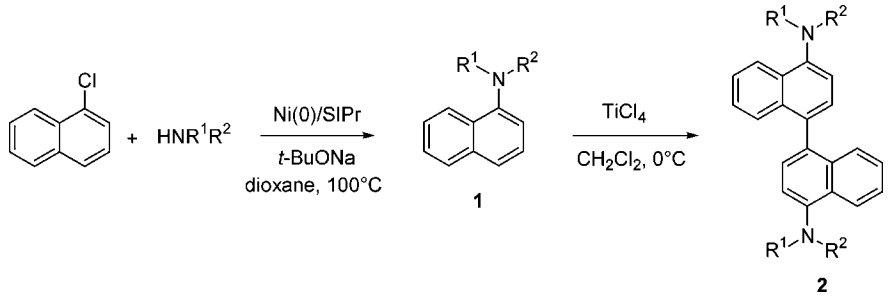

amination conditions [Ni(0) (5 mol %), SIPr (5 or 10 mol %), *t*-BuONa (150 mol %), dioxane, 100 °C] we developed.[14b,c]

As can be seen from Table 1, reactions performed with alicyclic amines (entries a and b) proceeded smoothly, affording the corresponding 1-naphthylamines **1** in good yields. For example, under the reaction conditions, pyrrolidine gave compound **1a** in 85% yield. Anilines gave results similar to those of alicyclic amines. Diarylation of the starting aniline could not be detected even after prolonged reaction times in the presence of an excess of 1-chloronaphthalene. The presence of two methyl groups at the ortho position of the aniline (entries d and e) has no deleterious effect. Using hindered amines such as 2,6-dimethylaniline or mesitylamine as substrates led to products **1d** and **1e** in, respectively, 82% and 81% yield. In every reaction, very little dechlorinated byproduct was observed (less than 5%).

We next turned our attention to the following step involving oxidative coupling of 1-naphthylamines **1** mediated by $TiCl_4$. In oxidative coupling of *N*,*N*-dimethylnaphthylamine, optimized reaction conditions have recently been reported.[9] When the homocoupling of compounds **1** was conducted with 1.5 equiv of $TiCl_4$ between 0 and 25 °C as described by Periasamy,[9] the corresponding naphthidines **2** were isolated in modest yields (26−33%). Careful attention to reaction conditions proved critical in order to obtain products **2** in good yields. Much better results (see Table 1) were obtained when the oxidative coupling and the hydrolysis of the reaction medium were both conducted between −5 and 0 °C. For example, the isolated yield of naphthidine **2a**, disubstituted by the pyrrolidino group, which among dialkylamino groups exhibits the most pronounced resonance effect and the strongest donor character,[16] could be improved from 26% to 76% when the whole coupling was performed between −5 and 0 °C. Except compound **1b**, the transformation was found to be general for all 1-naphthylamines **1** studied, and their isolation was easily achieved by column chromatography. Finally, 1-naphthylmorpholine **1b** failed to react under the reaction conditions. No side product was observed. This failure does probably not originate from the chelating properties of the oxygen atom toward Ti^{4+} since oxygen-containing substrates such as **1g** afforded the expected homocoupled product **2g** in high yields. Due to the electron-withdrawing effect of the oxygen atom,[17] it seems more likely that the nucleophilicity of the nitrogen atom is too weak to generate the aryl titanium and radical cation species involved in the oxidative coupling (Scheme 2).

SCHEME 2. Proposed Mechanism for the $TiCl_4$-Catalyzed Homocoupling of Compounds 1

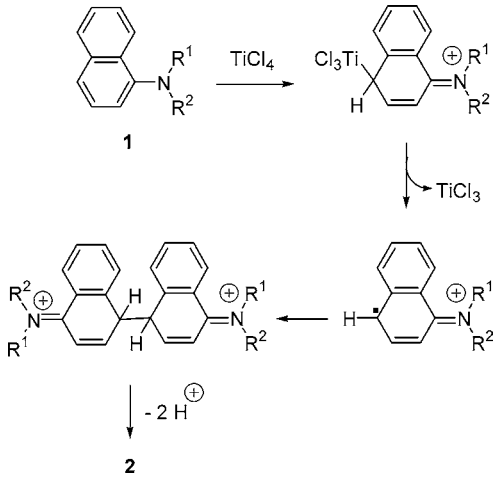

Electrochemical Studies. Cyclic voltammetry (CV) was used to characterize the electrochemical behavior of compounds **2a,c**−**h**. The measurements were carried out in acetonitrile at room temperature using tetrabutylammonium hexafluorophosphate (0.1 M) as the supporting electrolyte and a saturated Calomel electrode as the reference. CV experiments were performed at various scan rates extending from 10 mV s^{-1} to 2 V s^{-1}; within this whole range, all recorded voltammograms were characterized by peak currents directly proportional to the square root of potential scan rate, indicating that the electron-transfer processes involving compounds **2a,c**−**h** were diffusion-controlled.[18]

Typical CV curves are depicted in Figure 2 for compounds **2a**, **2c**, **2d**, and **2g**. All of the novel compounds **2a,c**−**h** exhibit a single, two-electron, reversible signal in the potential range 0.5−0.8 V (oxidation of the 1,1′-binaphthyl-4,4′-bispyrrolidine **2a** at 0.49 V and at ca. 0.7−0.8 V for *N*,*N*′-diaryl-(1,1′-binaphthyl)-4,4′-diamine **2c**−**h**), similarly to results reported for the related *N*,*N*,*N*′,*N*′-tetramethylnaphthidine (TMN) and *N*,*N*′-diphenylnaphthidine.[8−10] The electrochemical characteristics of compounds **2a,c**−**h** are summarized in Table 2. The lower oxidation potential of **2a** is due to the stronger donating properties of the pyrrolidinyl group compared to those of arylamines.[16] The two-electron-transfer process was confirmed by coulometry (Table 2), corresponding to the one-step forma-

(15) (a) Herrmann, W. A.; Reisinger, C. P.; Spiegler, M. *J. Organomet. Chem.* **1998**, *557*, 93. (b) Böhm, V. P. W.; Gstöttmayr, C. W. K.; Weskamp, T.; Herrmann, W. A. *J. Organomet. Chem.* **2000**, *595*, 186. (c) Bourissou, D.; Guerret, O.; Gabbaï, F. P.; Bertrand, G. *Chem. Rev.* **2000**, *100*, 39. (d) Herrmann, W. A. *Angew. Chem., Int. Ed.* **2002**, *41*, 1290.

(16) Brown, H. C.; Okamoto, Y. *J. Am. Chem. Soc.* **1958**, *80*, 4979.

(17) (a) Roberts, S. M.; Suschitzky, H. *J. Chem. Soc., Chem. Commun.* **1967**, 893. (b) Perepichka, I. F.; Popov, A. F.; Kostenko, L. I.; Piskunova, Zh. P. *Org. React.* **1986**, *23*, 317. (c) Hartwig, J. F.; Richards, S.; Baranavo, D.; Paul, F. *J. Am. Chem. Soc.* **1996**, *118*, 3626. (d) Beletskaya, I. P.; Bessmertnykh, A. G.; Guilard, R. *Tetrahedron Lett.* **1999**, *40*, 6393.

(18) Bard, A. J.; Faulkner, L. R., *Electrochemical Methods, Fundamentals and Applications*, 2nd ed.; John Wiley & Sons: New York, 2001.

TABLE 1. Synthesis of 1-Naphthylamines 1 and Naphthidines 2

Entry	Amine	Compound **1**	Yield (%)[a]	Compound **2**	Yield (%)[a]
a		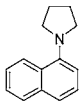	85	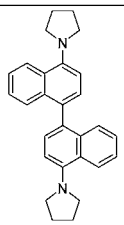	76
b		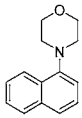	86	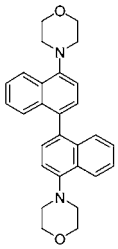	0
c		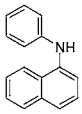	87	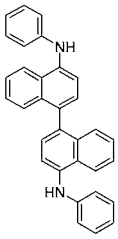	59
d	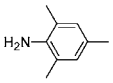	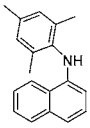	82	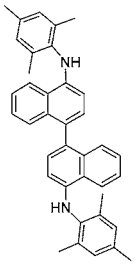	63
e		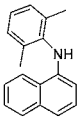	81	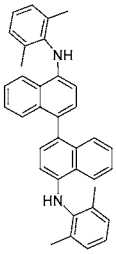	65
f		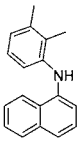	83	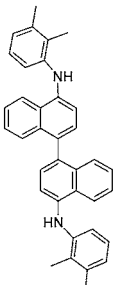	56

Table 1 (Continued)

Entry	Amine	Compound **1**	Yield (%)[a]	Compound **2**	Yield (%)[a]
g	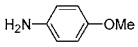	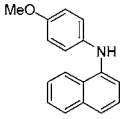	82	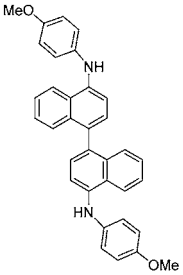	75
h	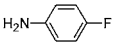	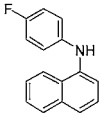	76	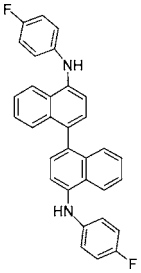	52

[a] All the yields refer to pure isolated products characterized by ^{1}H and ^{13}C NMR, IR and elemental analysis.

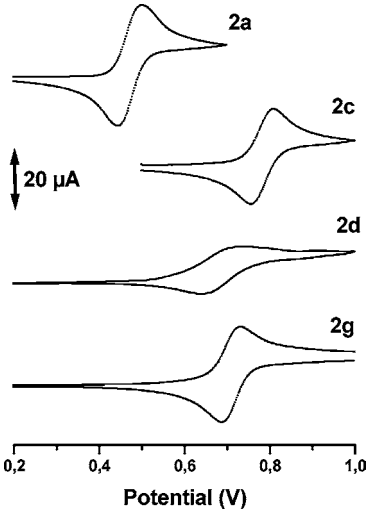

FIGURE 2. Cyclic voltammograms of compounds **2a**, **2c**, **2d**, and **2g** (1×10^{-3} M in acetonitrile containing 0.1 M Bu_4NPF_6) recorded at a potential scan rate of 20 mV s^{-1}.

tion of the dication $\mathbf{2}^{2.2+}$ (evidenced by several spectroscopic techniques, see below). The anodic-to-cathodic peak separation observed in CV, however, was in the range 40−60 mV, suggesting indeed the transfer of more than one electron, but it was not strictly equal to 30 mV (the theoretical value expected in case of two-electron-transfer processes).[18] This might be due to nonideal reversible behavior (electron-transfer kinetic limitations), which was more or less pronounced depending on the compounds (compare, e.g., **2d** and **2g** in Figure 2).

To further point out the two-electron process, even in the small time scale of the CV experiments, additional chronoamperometric measurements have been performed on derivative **2g** using an ultramicroelectrode (radius 50 μm) in conditions

TABLE 2. Electrochemical Characteristics of Compounds 2a,c−h

compound	E_{pa}[a]	E_{pc}[a]	i_{pa}/i_{pc}[a]	n[b]
2a	0.49	0.44	1.02	1.9
2c	0.80	0.75	0.99	2.2
2d	0.72	0.64	1.08	2.1
2e	0.73	0.69	1.05	1.9
2f	0.74	0.69	0.98	nm
2g	0.73	0.69	1.01	2.0
2h	0.68	0.62	0.97	nm

[a] E_{pa}, anodic peak potential; E_{pc}, cathodic peak potential; i_{pa}/i_{pc}, ratio of anodic-to-cathodic peak currents. Other conditions: 0.1 M Bu_4NPF_6 in CH_3CN, potential vs SCE, Pt electrode, 25°C, scan rate 20 mV/s.

where both linear and spherical diffusion are expected to occur successively and using the well-known ferrocene/ferricinium redox couple as a single-electron-transfer reference (see Supporting Information). They revealed a value of $n = 1.8 \pm 0.2$, confirming the two-electron transfer reaction in the early times of the electrochemical experiment. The chronoamperometric data also led to the evaluation of the diffusion coefficient of derivative **2g**, which was calculated as about 8×10^{-6} cm^2 s^{-1}, a value of the same order of magnitude as that reported for TMN.[19] Further evidence to support the reversible two-electron transfer in CV is given by the variation of peak currents of **2g** as a function of square root of scan rate, which is $2^{3/2}$ times higher than that of ferrocene (at the same concentration), according to the Randles−Sevcik equation,[17] after correction for the lower diffusion coefficient of **2g** with respect to that of ferrocene (2×10^{-5} cm^2 s^{-1}).[20,21]

The above results are consistent with a single reversible two-electron oxidation of **2** into a stable di(radical cation), $\mathbf{2}^{2.2+}$.

(19) Miras, M. C.; Silber, J. J.; Sereno, L. *J. Electroanal. Chem.* **1986**, *201*, 367.
(20) Martin, R. D.; Unwin, P. R. *J. Electroanal. Chem.* **1997**, *439*, 123.
(21) Ikeuchi, H.; Kanakubo, M. *Electrochemistry (Tokyo)* **2001**, *69*, 34.

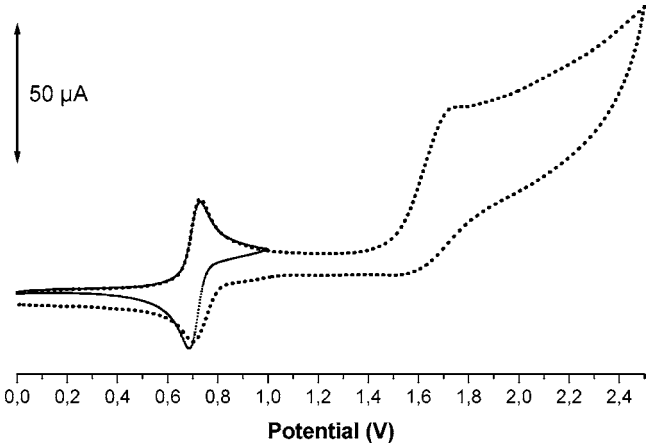

FIGURE 3. Cyclic voltammograms of compound **2g** recorded in two potential windows, at a scan rate of 50 mV s^{-1} (other conditions as in Figure 2).

This occurs probably via two successive electron transfers (EE mechanism) involving first the formation of the radical cation $\mathbf{2}^{\bullet+}$, which is then oxidized to $\mathbf{2}^{2.2+}$ at a potential value lower than that corresponding to the first electron transfer ($E°_2 < E°_1$), as previously suggested for the electrochemical oxidation of TMN.[19] Such situations where the second electron transfer is much easier than the first one can be indeed observed when, e.g., conformation changes are concerted with the electron transfer.[22] This will be discussed below from results obtained by theoretical calculations made on derivatives **2g**, $\mathbf{2g}^{\bullet+}$, and $\mathbf{2g}^{2.2+}$. The high stability of the di(radical cation) was also pointed out by thorough electrolysis monitored by linear scan voltammetry at rotating disk electrode at various completion levels of the reaction (see Supporting Information).

It should be noted finally that extending the potential scanning range up to the anodic limit (2.5 V) led to the observation of a second irreversible oxidation peak at about 1.7 V, only for compound **2g** (Figure 3), whereas all of the CV curves recorded with the other naphthidine derivatives did not display any additional well-defined signal.

Although no attempt was made to interpret this additional oxidation step of compound **2g**, it is likely that this could arise from the oxidation of the *p*-methoxyphenyl moieties.[23] This second oxidation has only little influence on the reversibility of the first oxidation peak at 0.73 V. These results also demonstrate that, under the applied conditions, the di(radical cation)s $\mathbf{2}^{2.2+}$ are stable and do not lead to, e.g., dimerization, as was generally observed in the course of the decomposition of arylamine radical cations.[24]

UV−Visible and EPR Spectra of Oxidized Species. Quantitative conversion of naphthidines **2** to their di(radical cation) could be achieved either by chemical oxidation with thianthrenium perchlorate ($ThClO_4$),[25] or phenyliodine(III)bis(trifluoroacetate) (PIFA).[26] PIFA is a weak oxidant for compounds **2**, whereas with $ThClO_4$ the oxidation process was accomplished immediately. However, absorption spectra of the PIFA-oxidized species do not differ from those of the $ThClO_4$-oxidized ones.

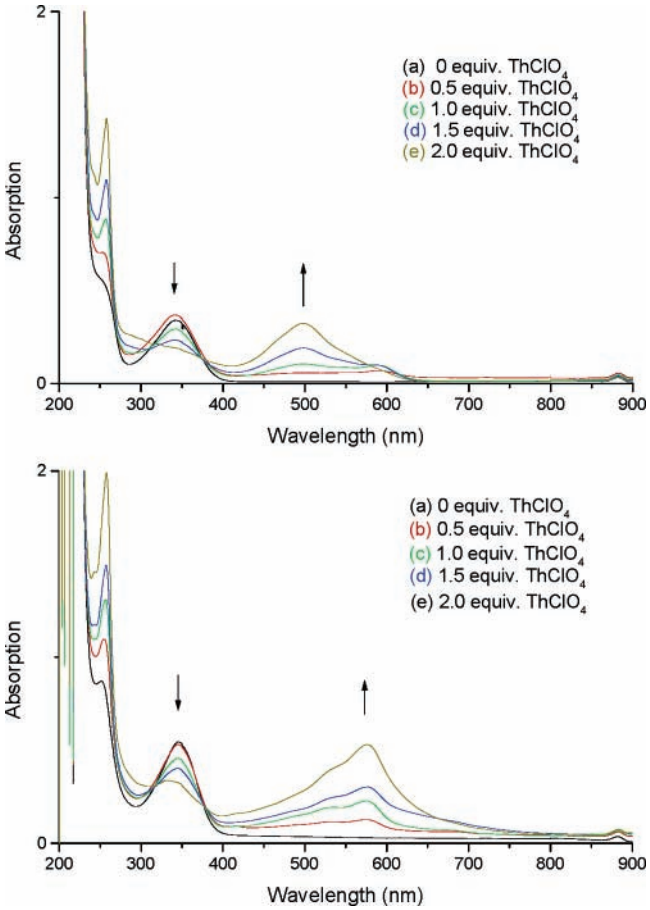

FIGURE 4. UV−vis spectra of the stepwise oxidation of **2a** (top) and **2g** (bottom) with $ThClO_4$ in $CHCl_3$ at 25 °C.

The oxidation of compounds **2a** and **2g** with $ThClO_4$ was monitored by UV−vis spectroscopy. A 0.1 mM solution of **2a** or **2g** in chloroform was treated repeatedly with 0.5 equiv of $ThClO_4$ in chloroform. Neutral **2** compounds were colorless in solution. With the addition of the oxidant, the solution turned immediately deep blue. Upon stepwise addition of $ThClO_4$, the absorption of neutral amine at λ_{max} = 341 and 345 nm, respectively, for **2a** and **2g** decreases and new bands appear at λ_{max} = 520 nm for **2a** and at 490, 537, and 577 nm for **2g** (Figure 4). The UV−vis absorption characteristics of the $ThClO_4$-oxidized species do not differ from those obtained when performing spectroscopic measurements in the course of the electrolytic transformation of **2a** and **2g** at various reaction times (Figure 5), indicating that the products generated by chemical oxidation were the same as those produced electrochemically. Note that the spectra of **2a** and **2g** after chemical oxidation showed a single additional band at ca. 255 nm owing to the presence of reduced $ThClO_4$. The appearing bands were ascribed to formation of $\mathbf{2}^{2.2+}$ and reached a maximum intensity after addition of exactly 2 equiv of $ThClO_4$, demonstrating the near quantitative formation of the di(radical cation) $\mathbf{2}^{2.2+}$ in which each naphthylamine unit carries an unpaired electron. This quantitative oxidation was also pointed out in the electrochemi-

(22) (a) Bellec, N.; Boubekeur, K.; Carlier, R.; Hapiot, P.; Lorcy, D.; Tallec, A. *J. Phys. Chem. A* **2000**, *104*, 9750. (b) Carlier, R.; Hapiot, P.; Lorcy, D.; Robert, A.; Tallec, A. *Electrochim. Acta* **2001**, *46*, 3269.

(23) Zweig, A.; Hodgson, W. G.; Jura, W. H. *J. Am. Chem. Soc.* **1964**, *86*, 157.

(24) Seto, E. T.; Nelson, R. F.; Fritsch, J. M.; Marcoux, L. S.; Leedy, D. W.; Adams, R. N. *J. Am. Chem. Soc.* **1966**, *88*, 3498.

(25) Murata, Y.; Shine, H. J. *J. Org. Chem.* **1969**, *34*, 3368. Caution! Thianthrenium perchlorate is a shock-sensitive solid that should be handled only on a small scale and with due care.

(26) Eberson, L.; Hartshorn, M. P.; Persson, O. *Acta Chem. Scand.* **1995**, *49*, 640.

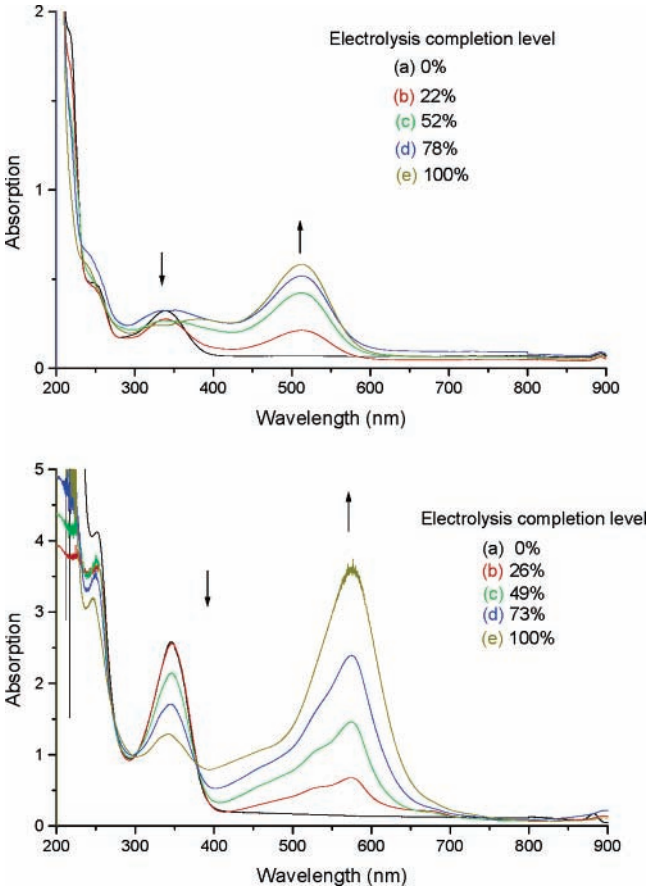

FIGURE 5. UV−vis spectra of the electrochemical oxidation of **2a** (top) and **2g** (bottom) in CH_3CN at 25 °C.

cal reactions, as 2 mol of electrons were necessary to complete the electrolyses. Upon further addition of $ThClO_4$ or by stirring the di(radical cation) at room temperature for 1 day, no further evolution in the absorption spectra was observed. In accordance with CV studies, this result illustrates the high stability of the generated di(radical cation) at room temperature and shows that no follow-up reaction such as dimerization occurs.

The corroborating evidence was obtained from the EPR spectrum of the oxidized solutions. Oxidation of **2g** by less than 1 or 2 molar equiv of $ThClO_4$ yields EPR-active solutions. When less than 1 equiv of $ThClO_4$ is added to a solution of **2g** in dichloromethane, the EPR spectrum of the deep blue solution at 25 °C reveals only a single broad line with a spectral width of ca. 6.6 G (data not shown). Apart from an increasing intensity, the same spectrum was observed using 2 equiv of $ThClO_4$. The spectra obtained suggest that $ThClO_4$ immediately oxidizes **2g** into $\mathbf{2g}^{2.2+}$ and that the mono(radical cation) $\mathbf{2g}^{\cdot+}$ cannot be obtained with this oxidant. Figure 6 displays the EPR spectrum of $\mathbf{2g}^{2.2+}$ at 100 K in a frozen CH_2Cl_2 matrix, which shows a similar pattern as at 25 °C but slightly wider (ca. 10.0 G). More noteworthy is that, in both samples, the triplet-allowed $\Delta m_s = \pm 2$ resonance[27] was not detected in a half-field region of the allowed $\Delta m_s = \pm 1$, clearly indicating that the dication behaves like a pair of independent radicals in doublet spin state.

(27) (a) Selby, T. D.; Blackstock, S. C. *J. Am. Chem. Soc.* **1999**, *121*, 7152. (b) Domingo, V. M.; Aleman, C.; Brillas, E.; Julia, L. *J. Org. Chem.* **2001**, *66*, 4058. (c) Ito, A.; Nakano, Y.; Kato, T.; Tanaka, K. *Chem. Commun.* **2005**, 403.

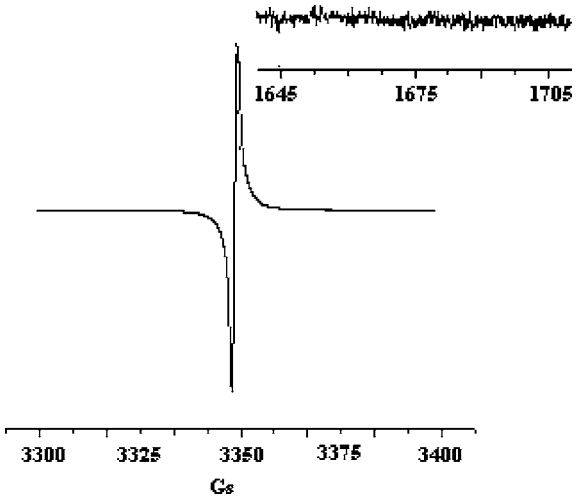

FIGURE 6. EPR spectra recorded at 100 K of **2g** oxidized by 2 equiv $ThClO_4$ in a frozen CH_2Cl_2 matrix.

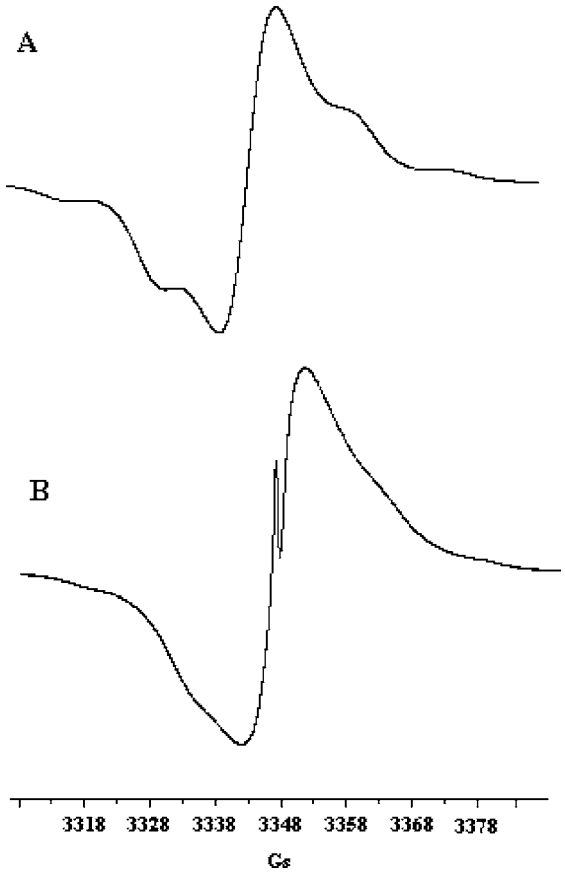

FIGURE 7. EPR spectra recorded at 100 K of (A) **2g** oxidized with 1 equiv of PIFA in CH_2Cl_2 and (B) **2g** oxidized with 2 equiv of PIFA in CH_2Cl_2.

When the oxidation was performed with 1 equiv of PIFA, a milder oxidant than $ThClO_4$, the oxidation of compound **2g** is slower. The EPR spectrum recorded at 100 K reveals five poorly resolved lines having a splitting constant of ca. 8.2 G (Figure 7A). Such a small hyperfine coupling constant is indicative of electron delocalization into the π-systems linked to the amino group.[28] The observed quintet spectrum is typical for benzidine cation radical with an unpaired electron equally coupled to two nitrogen atoms[29] and was attributed to the mono(radical cation)

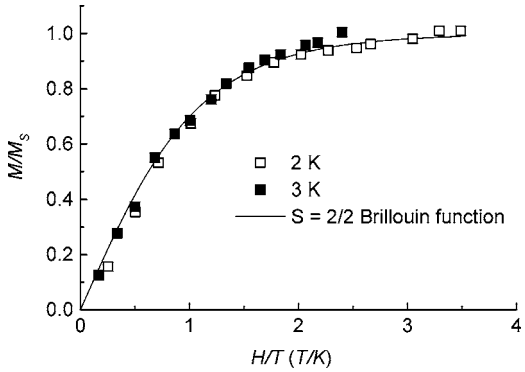

FIGURE 8. Normalized magnetization obtained at 2 K and 3 K as a function of H/T fitted by a $S = 2/2$ Brillouin function.

2g$^{\bullet+}$. The spectrum suggests therefore a fast intramolecular charge transfer between the neutral and singly oxidized naphthalene amine moieties of **2g**$^{\bullet+}$ or a delocalization of the unpaired electron over the whole system (see Theoretical Calculations), even at low temperature. After only 2 equiv of PIFA is added, the EPR spectrum gradually changes and the quintet signal is superimposed with the broad transition previously observed with $ThClO_4$ in dichloromethane (Figure 7B). No half-field $\Delta m_s = \pm 2$ absorption was observed, which verifies the doublet nature of the dication. Finally, the mono- and di-(radical cation)s generated from compound **2g** are stable at room temperature under aerobic conditions, displaying a qualitative half-life of, respectively, ca. 8 and 10 days. Actually, both **2g**$^{\bullet+}$ and **2g**$^{2.2+}$ were isolated from the CH_2Cl_2 solution by adding diethyl ether. However, we have not hitherto succeeded in obtaining single crystals suitable for the X-ray diffraction study.

Magnetization Measurements. Magnetization (M) of **2g**$^{2.2+}$ was measured using a PPMS/Quantum Design magnetometer. Raw data obtained were corrected from the sample holder. To take into account the diamagnetism of the solution, the same linear slope was also subtracted from the magnetizations measured at 2 K and 3 K so that magnetizations of **2g**$^{2.2+}$ are superimposed when they are plotted as a function of H/T. The normalized magnetizations (M/M_s) are depicted in Figure 8. The H/T dependence is very close to the Brillouin curve for $S = 2/2$, indicating the presence of triplet contribution to diradical **2g**$^{2.2+}$. The fraction of diradical in the triplet state is, however, very small. Indeed, the saturation magnetization amounts to roughly 2% of the signal expected when the whole solution is in the $S = 2/2$ state.

Theoretical Calculations

To gain a deeper understanding of the experimental trends, the molecular structures and electronic properties of the neutral and oxidized states of **2g** were theoretically investigated. Using the GAUSSIAN03 package,[30] ground state characterizations were performed within the density functional theory (DFT) approach using the gradient-corrected B3LYP hybrid exchange-correlation functional and the 6-31G* basis set (B3LYP/6-31G*). DFT calculations include electron correlation effects at a relatively low computational cost and the B3LYP exchange-correlation functional, which includes 20% Hartree−Fock exchange, is known to provide accurate equilibrium geometries.[31] The B3LYP XC functional has also been adopted in a number of recent investigations on radicals.[32] Nevertheless, two other well-known XC functionals (PBE0 and BHandHLYP) were also used in selected cases to test whether the B3LYP trends are robust. These other results summarized in Supporting Information lead to the same conclusions about the structural and electronic effects associated with the successive oxidations. The representation of the Kohn−Sham orbitals and spin densities has been performed using the MOLEKEL program.[33] Excitation energies for the neutral species have been evaluated using the MOSF code[34] at the ZINDO[35] level using the Mataga−Nishimoto−Weiss parametrization.

Neutral Compound. In the minimum energy conformation of the electronic ground state, the naphthyl groups define a torsion angle of 75.3°. This is slightly less than for the binaphthyl species where the dihedral angle amounts to 78.2°. On the other hand, this angle is more than twice larger than in the parent *N,N,N′,N′*-tetraphenylbenzidine (33.9°), which shows that the quasi perpendicular arrangement of the naphthyl units is induced by their extended nature. The bond lengths are essentially similar to those of the binaphthyl and, to a lower extent, of the naphthalene compound, the only difference being associated with the part of the naphthyl units that are influenced by the electron-donating NH-Ph groups (Figure 9). Moreover, the structure is not perfectly symmetric, and the bond lengths of the two naphthyl units can differ by as much as 0.001−2 Å. For simplicity, the values reported in Figure 9 are the averaged length of the equivalent bonds. As for the binaphthyl compound, there exists another equilibrium conformation. It has a similar

(28) Gerson, F.; Huber, W. *Electron Spin Resonance Spectroscopy of Organic Radicals*; Wiley-VCH: Weinheim, 2003; p 361.

(29) (a) Stamires, D. N.; Turkevich, J. *J. Am. Chem. Soc.* **1963**, *85*, 2557. (b) Dollish, F. R.; Hall, W. K. *J. Phys. Chem.* **1965**, *69*, 2127. (c) Seo, E. T.; Nelson, R. F.; Fritsch, J. M.; Marcoux, L. S.; Leedy, D. W.; Adams, R. N. *J. Am. Chem. Soc.* **1966**, *88*, 3498.

(30) Frisch, M. J.; Trucks, G. W.; Schlegel, H. B.; Scuseria, G. E.; Robb, M. A.; Cheeseman, J. R.; Montgomery, J. A., Jr.; Vreven, T.; Kudin, K. N.; Burant, J. C.; Millam, J. M.; Iyengar, S. S.; Tomasi, J.; Barone, V.; Mennucci, B.; Cossi, M.; Scalmani, G.; Rega, N.; Petersson, G. A.; Nakatsuji, H.; Hada, M.; Ehara, M.; Toyota, K.; Fukuda, R.; Hasegawa, J.; Ishida, M.; Nakajima, T.; Honda, Y.; Kitao, O.; Nakai, H.; Klene, M.; Li, X.; Knox, J. E.; Hratchian, H. P.; Cross, J. B.; Adamo, C.; Jaramillo, J.; Gomperts, R.; Stratmann, R. E.; Yazyev, O.; Austin, A. J.; Cammi, R.; Pomelli, C.; Ochterski, J. W.; Ayala, P. Y.; Morokuma, K.; Voth, G. A.; Salvador, P.; Dannenberg, J. J.; Zakrzewski, V. G.; Dapprich, S.; Daniels, A. D.; Strain, M. C.; Farkas, O.; Malick, D. K.; Rabuck, A. D.; Raghavachari, K.; Foresman, J. B.; Ortiz, J. V.; Cui, Q.; Baboul, A. G.; Clifford, S.; Cioslowski, J.; Stefanov, B. B.; Liu, G.; Liashenko, A.; Piskorz, P.; Komaromi, I.; Martin, R. L.; Fox, D. J.; Keith, T.; Al-Laham, M. A.; Peng, C. Y.; Nanayakkara, A.; Challacombe, M.; Gill, P. M. W.; Johnson, B.; Chen, W.; Wong, M. W.; Gonzalez, C.; Pople, J. A. *GAUSSIAN 03*, Revision B.04; Gaussian, Inc.: Pittsburgh, PA, 2003.

(31) Koch, W.; Holthausen, M. C. *A Chemist's Guide to Density Functional Theory*; Wiley-VCH: Weinheim, Germany, 2000.

(32) (a) Brown, E. C.; Borden, W. T. *J. Phys. Chem. A* **2002**, *106*, 2963. (b) Zhang, D. Y.; Hrovat, D. A.; Abe, M.; Thatcher Borden, W. *J. Am. Chem. Soc.* **2003**, *125*, 12823. (c) Bendikov, M.; Duong, H. M.; Starkey, K.; Houk, K. N.; Carter, E. A.; Wudl, F. *J. Am. Chem. Soc.* **2004**, *126*, 7416. (d) Serwinski, P. R.; Esat, B.; Lahti, P. M.; Liao, Y.; Walton, R.; Lan, J. *J. Org. Chem.* **2004**, *69*, 5247. (e) Kubo, T.; Sakamoto, M.; Akabane, M.; Fujiwara, Y.; Yamamoto, K.; Akita, M.; Inoue, K.; Takui, T.; Nakasuji, K. *Angew. Chem., Int. Ed.* **2004**, *43*, 6474. (f) Kwon, O.; Barlow, S.; Odom, S. A.; Beverina, L.; Thompson, N. J.; Zojer, E.; Bredas, J.-L.; Marder, S. R. *J. Phys. Chem. A* **2005**, *109*, 9346.

(33) Flükiger, P.; Lüthi, H. P.; Portmann, S.; Weber, J. *MOLEKEL 4.3*; Swiss Center for Scientific Computing: Manno, Switzerland, 2000−2002. Portmann, S.; Lüthi, H. P. *Chimia* **2000**, *54*, 766.

(34) *MOS-F* (semiempirical Molecular Orbital package for Spectroscopy, Fujitsu), V4, 1999.

(35) Ridley, J. E.; Zerner, M. C. *Theor. Chim. Acta* **1973**, *32*, 111. Martin, C. H.; Zerner, M. C. In *Inorganic Electronic Structure and Spectroscopy*; Solomon, E. I., Lever, A. B. P., Eds.; Wiley: New York, 1999; Vol. 1, p 555.

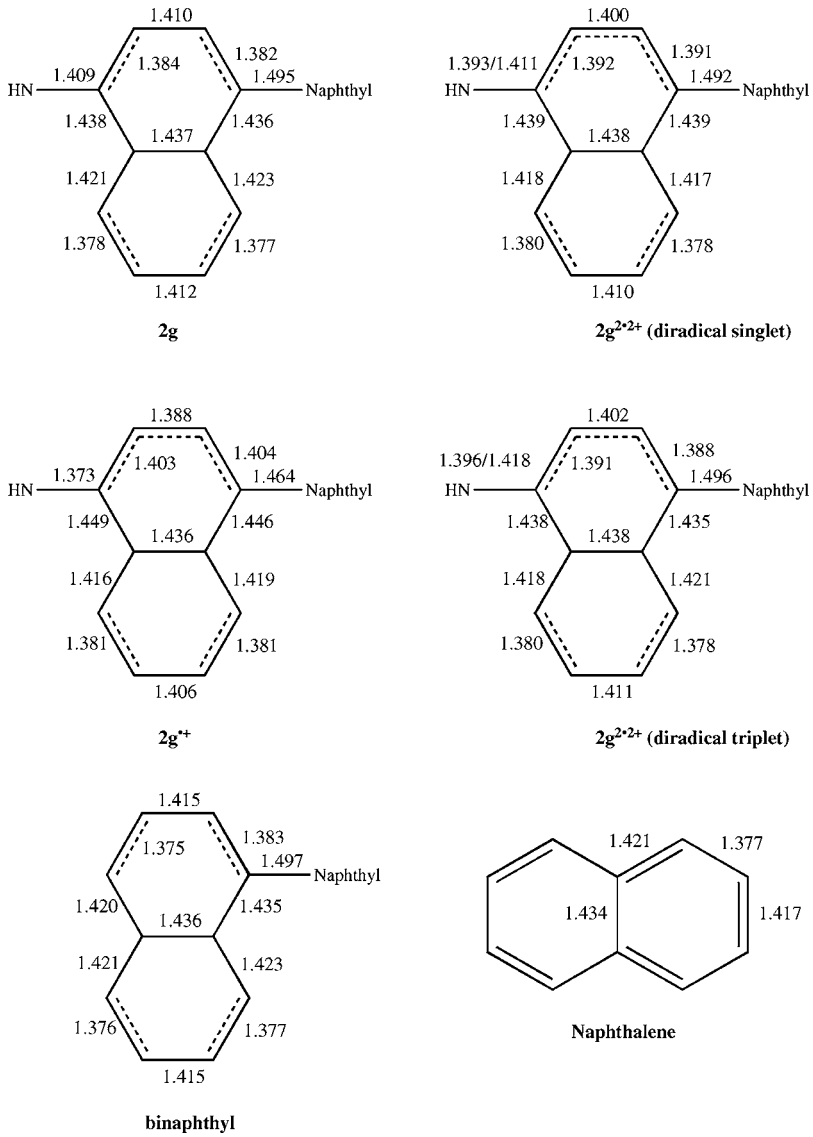

FIGURE 9. B3LYP/6-31G*-optimized bond lengths (Å) calculated for **2g** (neutral, closed-shell), **2g**$^{\bullet+}$ (radical cation, open-shell, doublet), **2g**$^{2.2+}$ (diradical dication, open-shell, singlet), **2g**$^{2.2+}$ (diradical dication, open-shell, triplet), binaphthyl, and naphthalene. Only the central part of the naphthidines is depicted.

energy ($\Delta E = 0.2$ kcal/mol) and a dihedral angle between the naphthyl units of 111.0°. The two conformations are characterized by quasi identical geometrical parameters. The large dihedral angles (75.3° or 111.0°) prevent electron delocalization between the two naphthylamine moieties. This is evidenced by the similarity between the geometrical parameters of **1g** and **2g**, as well as between their frontier orbitals. Figure 10 sketches the two highest occupied molecular orbitals (HOMOs) and two lowest unoccupied molecular orbitals (LUMOs) of **2g**. The HOMO and HOMO-1 of **2g** mimic the HOMO of **1g**, which is mostly localized on the MeO-Ph-NH part (see Supporting Information), with little delocalization between the two naphthylamine moieties. The LUMO of **1g** (see Supporting Information) is localized on the naphthyl unit so that in the course of the $TiCl_4$-mediated homocoupling, in- and out-of-phase combinations of the MOs of **1g** result in different MOs, at least in what concerns the junction between the naphthyl units.

The ZINDO calculations predict that the lowest-energy absorption band observed for **2g** at 345 nm (3.59 eV) is due to the second electronic excited state, which is estimated to lie

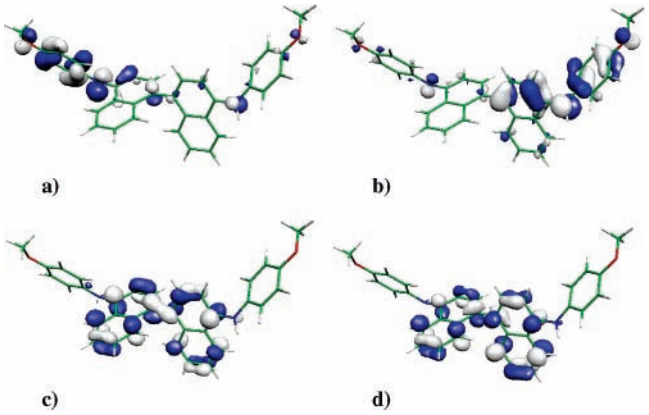

FIGURE 10. B3LYP/6-31G* Kohn−Sham orbitals (isocontour of 0.04 au) for **2g**: (a) HOMO-1, (b) HOMO, (c) LUMO, (d) LUMO+1.

3.81 eV (325 nm, $f = 0.841$) above the ground state and corresponds mainly to a HOMO−LUMO transition ($\epsilon_{HOMO} = -4.77$ eV, $\epsilon_{LUMO} = -0.98$ eV). For **1g**, the corresponding

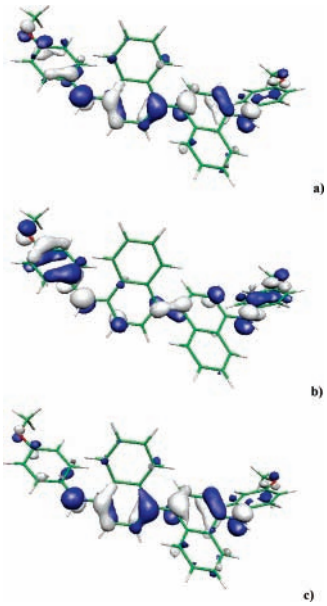

FIGURE 11. B3LYP/6-31G* Kohn−Sham orbitals (isocontour of 0.04 au) of $\mathbf{2g}^{\bullet+}$: (a) HOMO(α), (b) HOMO(*β*), (c) LUMO(*β*).

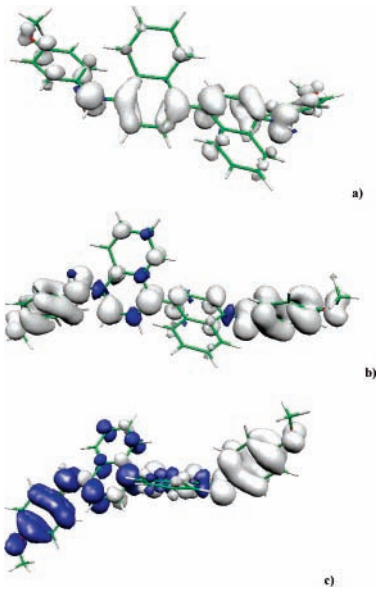

FIGURE 12. B3LYP/6-31G* spin densities (isocontour of 0.0015 au): (a) $\mathbf{2g}^{\bullet+}$, (b) triplet $\mathbf{2g}^{2.2+}$, (c) singlet $\mathbf{2g}^{2.2+}$.

quantities are 3.91 eV and 317 nm, showing again the weak electron delocalization between the two naphthyl units.

Radical Cation Compound. The minimum energy conformations of the electronic ground state are characterized by dihedral angles of 55.6° and 136.3°, with the former being 1.4 kcal/mol higher in energy. Following this reduction of the dihedral torsion angle by about 20°, the oxidation of **2g** is accompanied by an increase in quinonoïd character, which also results in a shortening of the inter-ring CC bond by 0.031 Å and of the CN bonds by 0.036 Å, as well as in the typical reversal of the bond lengths in the two rings of the naphthyl moieties that participate directly in the electron conjugation (Figure 9). In the parent *N*,*N*,*N*′,*N*′-tetraphenylbenzidine, removal of one electron leads also to a reduction of the torsion angle. It amounts to 14.6° to reach a torsion angle of 19.3°. Although in **2g** the MOs are localized on either side of the molecule, in $\mathbf{2g}^{\bullet+}$, they are delocalized over both units because of the increase in planarity. This is illustrated in the case of the HOMO(α), HOMO(*β*), and LUMO(*β*) (Figure 11a−c), which present the same pattern as their parent HOMO and HOMO-1 of **2g** and as their parent HOMO of **1g**. The spin density is distributed over the whole system (Figure 12a), whereas within the Mulliken population analysis scheme it presents maximum values of 0.14 |e| on the N atoms. The excess positive charge is also borne by all atoms of the system. The decrease in planarity when going from $\mathbf{2g}^{\bullet+}$ to **2g** can thus be related to the addition of an electron to the LUMO(*β*), which exhibits an antibonding inter-ring interaction.

Dication Compound. In the second oxidation step, the removed electron can originate either from the same MO as at the first oxidation step or from another MO. In the former case, a singlet closed-shell dication is formed, whereas the second situation corresponds to creating a diradical dication. B3LYP/6-31G* calculations predict that the singlet closed-shell system, which is characterized by an increased quinonoïd character [d_{CC} = 1.437 versus 1.495 Å and d_{CN} = 1.354 versus 1.409 Å for the neutral species] and a torsion angle of 41.5°, is less stable by about 4−5 kcal/mol than the diradical structures. This reduction of the torsion angle is related to the removal of the second electron from a MO presenting an antibonding inter-ring interaction. Then, two types of diradical species can be formed as a function of the spin pairing of the electrons: a singlet and a triplet state. The B3LYP/6-31G* calculations do not provide a definitive answer concerning the relative stability of the singlet and triplet diradical dication states because the energy difference for the corresponding optimized geometry is only 0.4 kcal/mol in favor of the singlet. This difference reaches 0.8 kcal/mol when correcting the singlet energy for spin contamination using the expression of Yamaguchi et al.[36] Then, keeping the geometries optimized for the isolated species while including solvent effects using the IEFPCM scheme[37] increases this difference to 1.3 kcal/mol, whereas performing a geometry optimization with the solvent gives a difference of 0.8 kcal/mol. The other XC functionals also predict that the singlet diradical is more stable than the triplet (PBE0, 3.56 kcal/mol; BHandHLYP, 1.87 kcal/mol), although the BHandHLYP value presents a larger spin contamination. On the other hand, the energy difference and the changes in geometrical parameters, as discussed later, being small, the unpaired electrons appear weakly coupled. Although the energy differences are very small, the most stable conformer for both the singlet and triplet diradicals presents a torsion angle larger than 90°: 122.0° for the singlet and 111.6° for the triplet. The other stable conformers have torsion angles of 67.7° and 75.1°, for the singlet and triplet, respectively. In addition to the torsion angle between the naphthyl units, the triplet diradical structure with an inter-ring CC bond length of 1.496 Å and NC distances of 1.407 Å resembles much that of the neutral compound (Figure 9). The quinonoïd character is stronger in the singlet diradical but still much weaker than in $\mathbf{2g}^{\bullet+}$ (Figure 9).

Starting from the radical cation, the triplet is obtained by removing the electron from the *β* HOMO, which exhibits a bonding interaction between the naphthyl moieties (Figure 11b). This explains the increase in the torsion and the reduction in

(36) Yamaguchi, K.; Jensen, F.; Dorigo, A.; Houk, K. N. *Chem. Phys. Lett.* **1988**, *149*, 537.

(37) See, for instance: Tomasi, J.; Cammi, R.; Mennucci, B.; Cappelli, C.; Corni, S. *Phys. Chem. Chem. Phys.* **2002**, *4*, 5697 and references therein.

the quinonoïd character. On the other hand, the structure of the singlet diradical is essentially explained starting from the neutral species where both the HOMO and HOMO-1 are doubled, one of each spin type on each moiety of the naphthidine and where the electrons on the α HOMO-1 and β HOMO-1 are removed (Figure 10a). The spin density topology substantiates this explanation because the larger amplitudes are now located on the NH-Ph-OMe parts of the system (Figure 13c), whereas the corresponding HOMOs and LUMOs present related topologies (see Supporting Information).

Properties. When accounting for solvent effects within the IEFPCM scheme,[37] the first ionization energy, which corresponds to the transition between the neutral and radical cation compounds, amounts to 4.44 eV. The second ionization energy to form the di(radical cation) is slightly larger and attains 4.93 eV. The small difference between the two ionization energies explains why the CV exhibits a single, two-electron signal. More details can be found in Supporting Information.

Conclusions

In conclusion, naphthidines **2**, easily available by a nickel-catalyzed aryl amination reaction between 1-chloronaphthalene and amines followed by $TiCl_4$-mediated oxidative coupling, represent a new class of easily oxidizable compounds. Cyclic voltammetry, coulometric measurements, and EPR reveal that naphtidines **2** exhibit good donor properties, showing a single two-electron oxidation wave to form the di(radical cation) species $\mathbf{2}^{2.2+}$ that display remarkable stability at room temperature in solution and in the solid state. Such stability is an important factor when considering potential applications of these compounds, especially in OLEDs.

The oxidation process has been theoretically studied by optimizing the structures of the monocation and dication species arising from naphthidine **2g**. The important conformational changes of **2g** upon oxidation account for its electrochemical properties. DFT theoretical calculations predict that the first oxidation of compound **2g** into $\mathbf{2g}^{\bullet+}$ is accompanied by an important decrease of the torsion angle between the two naphthyl moieties, which results in an increase of the quinoid character, while the second oxidation into $\mathbf{2g}^{2.2+}$ partially restores the large torsion angle and the aromatic character. The coalescence of the two oxidation peaks is therefore attributed to the structural rearrangement that accompanies the redox process.

Through magnetization experiments, we have finally shown that the di(radical cations) $\mathbf{2}^{2.2+}$ have an energetic preference for spin pairing yielding a singlet diradical ground state.

Experimental Section

General Procedure 1. Coupling of 1-Chloronaphthalene with Secondary Cyclic Amines. The average yields for each reaction are shown in Table 1. A typical procedure is given for entry 1.

1-(1-Naphthyl)pyrrolidine[38] (1a). A 50 mL Schlenk tube was loaded with degreased NaH (16 mmol), $Ni(acac)_2$ (0.5 mmol, 5 mol %), SIPr·HCl (0.5 mmol, 5 mol %), and 6 mL of dioxane, and the mixture was heated to reflux. A solution of *t*-BuOH (15 mmol) in 3 mL of dioxane was then added dropwise followed by the amine (15 mmol), and the mixture was further stirred for 0.5 h. A solution of 1-chloronaphthalene (10 mmol) in 3 mL of dioxane was then added, and the reaction was monitored by GC. After complete consumption of the aryl chloride, the mixture was cooled to room temperature and adsorbed onto silica gel. The crude reaction mixture was purified by silica gel chromatography to furnish compound **1a** as a pale yellow oil (85%). ^{1}H NMR (400 MHz, $CDCl_3$) δ 7.76−7.74 (m, 2H), 7.67−7.65 (m, 1H), 7.53−7.49 (m, 1H), 7.44−7.38 (m, 2H), 6.90 (d, J = 7,20 Hz, 1H), 3.30−3.28 (m, 4H), 1.94−1.92 (m, 4H); ^{13}C NMR (100 MHz, $CDCl_3$) δ 143.8, 130.2, 128.1, 127.1, 126.5, 125.6, 124.1, 121.2, 111.3, 52.5, 24.5. MS m/z = 197.

General Procedure 2. $TiCl_4$-Mediated Oxidative Coupling of Naphthylamines 1. The average yields for each reaction are shown in Table 1. A typical procedure is given for entry 1.

1,1′-Binaphthyl-4,4′-bis-pyrrolidine (2a). A solution of 1-(1-naphthyl)pyrrolidine **1a** (5 mmol) in anhydrous CH_2Cl_2 (5 mL) was chilled to −5 °C under nitrogen. $TiCl_4$ (1.7 mL of 1:1 solution of $TiCl_4/CH_2Cl_2$, 7.7 mmol) was added dropwise for 5 min. The reaction mixture was stirred at −5 °C for 1 h and stirred further at 0 °C for 8 h. A saturated K_2CO_3 solution (10 mL) was then added, and the mixture was stirred for 0.5 h at 0 °C. The layers were separated, and the aqueous layer was extracted with CH_2Cl_2 (2 × 15 mL). The organic layers were combined, washed with brine solution (5 mL), dried over $MgSO_4$, and concentrated. The crude reaction mixture was purified by silica gel chromatography to furnish **2a** as a yellow solid (76%). Mp = 177 °C. ^{1}H NMR (400 MHz, $CDCl_3$) δ 8.30 (d, J = 8.3 Hz, 2H), 7.42−7.33 (m, 6H), 7.24−7.20 (m, 2H), 7.06 (d, J = 7.6 Hz, 2H), 3.42 (m, 4H), 2.05 (s, 4H); ^{13}C NMR (100 MHz, $CDCl_3$) δ 147.3, 134.4, 132.1, 128.2, 128.1, 127.1, 125.4, 124.7, 124.1, 111.2, 52.8, 24.8. Anal. Calcd. for $C_{28}H_{28}N_2$: C, 85.67, H, 7.19, N, 7.14. Found: C, 85.59, H, 6.95, N, 7.46.

Acknowledgment. The authors would like to thank Pr. André MERLIN (LERMAB, Université Henri Poncaré, Nancy 1) for EPR spectra. B.C. thanks the Belgian National Fund for Scientific Research for his Research Director position. The calculations were performed on the Interuniversity Scientific Computing Facility (ISCF), installed at the Facultés Universitaires Notre-Dame de la Paix (Namur, Belgium), for which the authors gratefully acknowledge the financial support of the FNRS-FRFC and the "Loterie Nationale" for the convention no. 2.4578.02, and of the FUNDP.

Supporting Information Available: General experimental information, experimental procedures, characterization data of compounds **1a**−**h** and **2a**−**h**, chronoamperometry of naphthidines, dependence of anodic-to-cathodic peak potentials on scan rate at different concentrations of naphthidine **2g**, voltammetric in situ monitoring of the electrolysis of compound **2g**, UV−visible spectra of the stepwise chemical oxidation of compounds **2c**−**f** and **2h**, and computational details. This material is available free of charge via the Internet at http://pubs.acs.org.

JO0517444

(38) Srinivas, G.; Periasamy, M. *Tetrahedron Lett.* **2002**, *43*, 2785.